

Densification of Ca-doped alumina nanopowders prepared by a new sol-gel route with seeding

Atsushi Odaka <sup>a</sup>, Tomohiro Yamaguchi <sup>a,\*</sup>, Takayuki Fujita <sup>b</sup>, Seiichi Taruta <sup>a</sup> and Kunio Kitajima <sup>a</sup>

<sup>a</sup> Department of Chemistry and Material Engineering, Faculty of Engineering, Shinshu University, 4-17-1 Wakasato, Nagano-shi, 380-8553

<sup>b</sup> Taimei Chemicals Co. Ltd., Minamiminowa-mura, Kamiina-gun, Nagano, 399-4597

\*Corresponding author:

Tomohiro Yamaguchi

E-mail: [mtmouth@shinshu-u.ac.jp](mailto:mtmouth@shinshu-u.ac.jp)

Tel: +81-26-269-5417

Fax: +81-26-269-5415

## Abstract

This paper demonstrates that the Ca-doped alumina nanopowders prepared by a new sol-gel route using polyhydroxoaluminum (PHA) and  $\text{CaCl}_2$  solutions under  $\alpha$ -alumina seeding represent a viable option for producing fine-grained ceramics. Appropriate conditions for producing Ca-doped alumina nanopowders suitable for low-temperature finer-grained densification were 0.10 mol% Ca-doping, 5 mass%  $\alpha$ -alumina seeding and a calcination temperature of 900°C. These conditions led to the formation of new nano-sized alumina powders, which consisted of ~80 nm  $\alpha$ -alumina particles and  $\gamma$ -alumina nanoparticles. Using these Ca-doped nanopowders, fully densified alumina ceramics with a uniform microstructure composed of fine grains with an average grain size of 0.66  $\mu\text{m}$  could be obtained at 1375°C. Clearly, the Ca-doped nanopowders obtained here through the proposed sol-gel route are very suitable for fabricating dense, fine-grained alumina ceramics because an undoped sample with 5 mass% seeds led to a microstructure with an average grain size of 1.39  $\mu\text{m}$  at 1375°C.

Keywords: A. Sintering; A. Sol-gel process; B. Grain size; D.  $\text{Al}_2\text{O}_3$ ; Ca-doping

## 1. Introduction

Alumina ceramics are important in many fields of modern industry because of their excellent mechanical, electrical and optical properties, which are determined by their microstructure (grain size). The refinement of alumina powder processing techniques is key to obtaining a fine-grained microstructure. Recently, nanopowders such as transition alumina,<sup>1,2</sup> Mg<sup>2+</sup> cation doped  $\gamma$ -alumina<sup>3</sup> and nano-grained  $\alpha$ -alumina<sup>4-6</sup> powders have attracted much attention due to their intrinsic nanocrystalline nature. These powders can be synthesized by various routes.<sup>3,4,6-10</sup>

We have shown that the use of M<sup>2+</sup>-doped  $\gamma$ -aluminas synthesized through a polyhydoroaluminum (PHA) sol-gel process were very effective for obtaining a fine grain size upon sintering due to an intimate mixing of dopants at an atomic level.<sup>3,11</sup> Among the divalent cation dopants reported in our previous study, Ca<sup>2+</sup> is by far the best dopant for suppressing the grain growth of  $\alpha$ -alumina upon heating.<sup>11</sup> However, the low intrinsic nucleation density in such PHA-derived  $\gamma$ -alumina powders inevitably leads to a large isolation between nucleation sites, resulting in the formation of a vermicular microstructure.<sup>12,13</sup> Thus, to obtain dense, fine-grained alumina ceramics from M<sup>2+</sup>-doped  $\gamma$ -alumina powders at low temperatures, the formation of a vermicular microstructure must be hindered. This may be accomplished by the addition of  $\alpha$ -alumina seeds to provide multiple low-energy sites for nucleation,<sup>13</sup> which allows early impingement of the growing  $\alpha$ -alumina colonies, and hence, full densification at lower temperatures.

The present study focuses on the densification of Ca-doped alumina nanopowders obtained through the PHA sol-gel route with seeding. The powders consisted of mixtures of nanoparticles of ~80 nm  $\alpha$ -alumina and

$\gamma$ -alumina, whose  $\alpha$ - and  $\gamma$ -alumina content varied depending on the calcination conditions of the gels. The use of PHA-derived  $\gamma$ -alumina powders,<sup>3,14-16</sup> which are inherently agglomerated, limits the homogeneity of the seed distribution attainable when a dry process is employed for seeding. Thus, seeding was performed during the PHA sol-gel process. The use of planetary milling for the calcined powders allowed further deagglomeration, enhancing the homogeneity of the particle distribution in the starting powders.

The objectives of the present investigation are (i) to investigate the densification behavior of high-purity Ca-doped nanopowders obtained through sol-gel using a PHA solution under seeding by conventional pressureless sintering, rather than a pressure sintering method such as the pulse electric current sintering (PECS) method reported previously,<sup>3,14-16</sup> and (ii) to demonstrate the suitability of PHA-derived nanopowders as starting raw powders for achieving full densification with a finer-grained microstructure at lower temperatures.

## 2. Experimental

A high-purity PHA solution having an  $\text{Al}_2\text{O}_3$  concentration of 23.7 mass% and OH/Al ratio of 2.50 was prepared by dissolving Al metal in HCl solution;<sup>17</sup> the solution was prepared by dissolving high-purity Al metal (99.99%) in 9.6 mass% hydrochloric acid by heating gradually up to 90°C for about 10 h. Special attention was paid to the impurities. The  $\text{CaCl}_2 \cdot 2\text{H}_2\text{O}$  (Wako Pure Chemical Industries, Japan) used as a Ca source was dissolved in distilled water. The  $\alpha$ -alumina powder used for seeding was prepared from commercial  $\alpha$ -alumina powder (TM-DAR, Taimei Chemicals, Japan) by

planetary ball milling in ethanol for 24 h. The  $\text{CaCl}_2$  solution was added to the PHA solution under an  $\alpha$ -alumina seed content of 0-20 mass% to form a 0.10 mol%  $\text{Ca}^{2+}$  against the mole of  $\text{Al}_2\text{O}_3$  obtained from the PHA solution. As control sample, a seeded PHA solution was prepared without adding Ca-dopant solution.

The solution mixtures were stirred thoroughly and ultrasonicated. Then, the seeded sols were rapidly dried to prevent segregation of seeds. The resultant gels were ground into  $<150\ \mu\text{m}$  powders using a high-purity alumina mortar and pestle and then calcined at 500-900°C for 3 h. The calcined powders were deagglomerated again by planetary ball milling in ethanol, followed by slip casting into disks ( $\phi$ : 13 mm,  $t$ :  $\sim 3$  mm). The milled powders obtained at a calcination temperature of 900°C will hereafter be abbreviated as PA-S-Ca and PA-S for the PHA-derived alumina powder with and without Ca-dopant, respectively. Part of the PA-S-Ca and PA-S powders was uniaxially pressed at 300 MPa for comparison. The amounts of impurities (by mass), as measured by ICP after dissolution, in, for example, PL-S-Ca, were 23 ppm Si, 4 ppm Na, 4 ppm Mg and 26 ppm Fe, showing that the purity was higher than 99.99%. To determine the phase transformation temperature, DTA (TG8120: Rigaku Co., Ltd.) measurements were conducted at a heating rate of 10°C/min under flowing air, using 25-mg samples. The phases before and after calcination and the  $\alpha$ -fraction were determined by XRD using monochromatic  $\text{CuK}\alpha$  radiation (RINT2000 : Rigaku Co., Ltd.). The disk-shaped samples obtained by slip casting were sintered at 1200-1500°C for 1 h in air. A heating rate of 50°C/min (below 1300°C) and 12°C/min (above 1300°C) was employed, paying special attention to preventing overshoot at the predetermined sintering temperature.

The bulk density of the sintered samples was measured by the Archimedes method. The raw powders and the microstructure of their sintered specimens were characterized by a S-3100H scanning electron microscope (SEM) and a JEM 2010 transmission electron microscope (TEM). The samples were prepared by suspending the powders in ethanol and evaporating a droplet of the suspension onto a microgrid. The average grain size of the powders was measured one by one, and the arithmetic average was taken. The average grain size of the sintered samples was estimated by the line-intercept method using at least 100 grain measurements.

### 3. Results and discussion

#### 3.1 Preparation of Ca-doped alumina nanopowders

Figure 1 shows a TEM photograph of the seed powders. The average grain size of the seeds is  $\sim 75$  nm, however, there is some agglomeration of the seeds. In addition, there is trace amount (estimated to be  $\sim 6\%$  at most) of smaller agglomerated particles, which probably originated from the abrasion powders from the high-purity alumina milling media. The average size of the seed particles, as determined from the specific surface area ( $24.7 \text{ m}^2/\text{g}$ ), was 61 nm, in good agreement with the value estimated from the TEM micrograph. This shows that planetary milling is effective in deagglomerating and reducing the grain size of the starting TM-DAR powders since the average grain size of the TM-DAR powder was 120 nm (determined by TEM).

In the  $\gamma$ -alumina powder matrix obtained at  $500^\circ\text{C}$  from the PHA gel under 5% seeding, the approximate seed frequency was estimated to be  $\sim 3.5 \times 10^{14}$  seeds/ $\text{cm}^3$ , on the basis of the  $\gamma$ -alumina theoretical density of  $3.2 \text{ g}/\text{cm}^3$ .

Table 1 summarizes the powder characteristics of the seed and PA-series powders used for sintering. PA-S and PA-S-Ca powders calcined at 900°C transformed to ~90%  $\alpha$ -Al<sub>2</sub>O<sub>3</sub>, whereas the samples calcined at 800°C and 600°C had an  $\alpha$ -fraction of 65% and 40%, respectively.

A seed content of only 1 mass% decreased the exothermic DTA peak temperatures ( $T_P$ ) dramatically, from 1151°C to 977°C, showing the significant effect of seeding on the transformation. As the seed content increased,  $T_P$  gradually dropped to 955°C at a seed content of 5 mass%, nearly reaching saturation at 10 mass%. The difference in  $T_P$  ( $\Delta T$ ) between 0 mass% and 5 mass% was 196 K, while the  $\Delta T$  between 0 mass% and 1 mass% was 174 K. On the basis of these results, a seed content of 5 mass% was selected for the sol-gel process.

Figure 2 plots the  $\alpha$ -alumina fraction against calcination temperature for the PA-series powders. While the non-seeded sample showed a rapid increase in  $\alpha$ -fraction at a higher temperature of around 1000°C, the  $\alpha$ -alumina fraction of seeded samples increased in the lower temperature range of 500-900°C as the seed content increased from 1 to 5 mass%. Moreover, 0.1 mol% Ca-doping reduced the  $\alpha$ -alumina fraction, especially around 800°C, however, the  $\alpha$ -fraction almost reached the value for PA-S (~90%), i.e., the non-Ca-doped sample, at 900°C for 1 h.

The TEM micrographs of PA-S and PA-S-Ca powders calcined at 900°C (Fig. 3) demonstrate that the average grain size of  $\alpha$ -alumina particles is ~80 nm and that the PA-S and PA-S-Ca powders used for sintering have similar nanoparticle size distributions.

Preliminary experiments showed that lower calcination temperatures such as 600°C are effective in reducing the  $\alpha$ -alumina grain size, however, the

lower  $\alpha$ -fraction in the starting powders resulted in a marked increase in the sintering temperature to attain full density. Moreover, Ca-doping above 0.20 mol% was not effective because the suppression effect on grain growth was saturated and the undesirable secondary phase  $\text{CaAl}_{12}\text{O}_{19}$  precipitated at the higher temperatures  $>1400^\circ\text{C}$ . The critical concentration for secondary phase formation depended on the dopant content and the grain size developed.<sup>18</sup> All the powder samples studied here were intrinsically nano-sized alumina powders although they did not consist of a single phase. However, the powders calcined at  $800\text{-}900^\circ\text{C}$ , especially the PA-S-Ca powder calcined at  $900^\circ\text{C}$ , exhibited excellent sinterability, as discussed in the next section.

### 3.2 Fabrication of fine-grained alumina ceramics

The densification curves of the PA-S and PA-S-Ca powders are shown in Fig. 4. The PA-S samples sintered to 96.9% relative density at  $1300^\circ\text{C}$  and reached 99.1% at  $1375^\circ\text{C}$ . The PA-S-Ca powder sintered to 94.2% relative density at  $1300^\circ\text{C}$ , lower than that of the PA-S powder due to the presence of the Ca-dopant, however, reached  $>99.1\%$  at  $1375^\circ\text{C}$ . Thus, a  $>95\%$  density should be obtainable by sintering around  $1300^\circ\text{C}$  for longer periods of time.

The commercial  $\delta(35\%)/\alpha$ -alumina(65%) mixture sintered to only 88% relative density at  $1400^\circ\text{C}$ , with higher grain growth.<sup>1</sup> On the other hand, the PA-S-Ca(800) powders, which were calcined at  $800^\circ\text{C}$  and have a comparable  $\alpha$ -alumina fraction, sintered to  $>99\%$  relative density at  $1400^\circ\text{C}$ . This suggests that the PA-S-Ca powders have higher sinterability than the commercial  $\delta/\alpha$ -alumina powder because the  $\alpha$ -alumina nanoparticles in the former case was finer. This also demonstrates that the enhanced nano-sized nature of  $\alpha$ -alumina particles in the PA-S-Ca powders is the key to



low-temperature densification.<sup>4</sup>

Figure 5 shows SEM fractographs of PA-S and PA-S-Ca samples sintered at 1200°C. All of the samples have completely transformed into  $\alpha$ -alumina and undergone only slight grain coarsening, largely retaining their nanoparticle nature. The grain morphologies appear to be more equiaxed at the higher seed concentration of 5 mass% with Ca-doping. The  $\alpha$ -alumina grain size slightly decreased with Ca-doping, although the numbers of entrapped pores in the sintered specimens was somewhat larger.

The microstructure of PA-S and PA-S-Ca samples sintered at 1300-1400°C are shown in Fig. 6. The samples were polished and thermally etched before observation. The samples sintered to high densities and developed equiaxed grains. A homogenous fine-grained (0.75  $\mu\text{m}$ ) microstructure was obtained at 1400°C from PA-S-Ca nanopowders, while the microstructure of the commercial  $\delta(35\%)/\alpha$ -alumina(65%) powder sintered at 1400°C was reported to exhibit a broad grain size of 0.2-2.0  $\mu\text{m}$  grains with a few large pores.<sup>1</sup> In addition, Li and Ye<sup>6</sup> reported that the alumina nanoceramics obtained from  $\alpha$ -alumina nanopowders exhibited a much finer grain size of about 90 and 150 nm at 1450°C and 1500°C, respectively, however, the relative densities remained less than 95%. Thus, it is concluded that PA-S-Ca powders are very effective for achieving low-temperature full densification and a finer microstructure without abnormal grain growth.

Both PA-S and PA-S-Ca samples yielded high densities at 1400°C, however, sintering at 1500°C resulted in drastic grain growth, exhibiting different morphology of equiaxed grains for PA-S and elongated grains for PA-S-Ca. The PA-S-Ca sample also showed a broad grain size distribution (1-10  $\mu\text{m}$ ), which resulted from abnormal grain growth. This feature of microstructural

evolution is very similar to that of Ca-doped aluminas at 1500-1600°C reported by Altay and Gülgün<sup>19,20</sup> although the relative density of their samples was 96.5-98.5%. It has been reported that above a certain grain boundary concentration calcium is responsible for elongated grain morphology in  $\alpha$ -alumina.<sup>19,20</sup> The purity of the PA-S-Ca powder in the present study is high (>99.99%), however, only a small amount of Si impurity (23 ppm) might also enhance the formation/growth of elongated grains by co-doping effect.<sup>19-22</sup> Therefore, it should be a noticeable feature of the PA-S-Ca samples that almost full densification has been attained at lower temperature of 1375°C before triggering abnormal elongated grain growth. The elongated morphology is believed to be due to preferential segregation of Ca to basal plane in alumina grain boundary.<sup>19</sup>

As in the case of seeded boehmite,<sup>23-25</sup> the number frequency and dispersion homogeneity of  $\alpha$ -alumina seeds in PA-S and PA-S-Ca precursor gels is the key parameter controlling the size of the  $\alpha$ -alumina grains, which in turn significantly affects the low-temperature sintering behavior. Thus, the low-temperature densification behavior of PA-S-Ca powders forming a finer-grained microstructure is the result of the synergistic effect between the  $\alpha$ -alumina nanoparticles and Ca-dopant, which segregates to the grain boundaries during the transformation/sintering and hinders grain growth, leading to low-temperature full densification and a finer-grained microstructure. The grain size developed plays a key role to determine the level of calcium segregation at the grain boundaries<sup>19,20</sup> and the grain boundary structure.<sup>26</sup>

The average grain size is plotted against sintering temperature in Fig. 7. The average grain size of PA-S samples increased up to 1400°C, followed by

drastic increase at 1500°C. Meanwhile, the average grain size of the PA-S-Ca sample increased gradually up to 1400°C, reaching a grain size of only 0.75  $\mu\text{m}$  with retaining homogeneous microstructure. This clearly shows the retarding effect of the Ca-dopant, which was distributed homogeneously in the sintering powder matrix. However, as mentioned above, elongated abnormal grain growth occurred abruptly at 1500°C, and thus slightly decreasing the relative density at higher temperatures.

Our preliminary study showed that Ca-doping level had only a slight effect on the  $\alpha$ -alumina particle size when calcination was performed at 900°C. This shows that the suppression effect of the Ca-dopant occurred itself mainly in the sintering stage of the densification process up to 1400°C, during which the Ca-dopant segregated to the grain boundaries, thereby retarding grain growth due to solute drag effect of segregated Ca on the grain boundary mobility. The PA-series powders obtained at the calcination temperature of 600°C had poorer sinterability. This resulted from the high  $\gamma$ -alumina content, although the average grain size developed was slightly smaller than that obtained using the PA-series powders obtained at 900°C.

For comparison, a green pellet of the PA-S-Ca sample obtained by uniaxial pressing was sintered at 1400°C under the same sintering conditions. A relative density of 98.3% was obtained. This was lower than the density obtained by slip casting (99.2%), which indicated the advantage of slip casting over uniaxial pressing as a forming method. This presumably resulted from the large residual pores in the green body of the uniaxially pressed samples because some large agglomerates tended to persist due to the use of the slurry drying process. Li and Ye<sup>6</sup> pointed out that, in pressureless sintering, a green body having a higher density and smaller

pores easily densified into a dense nanoceramic when sintered at the same temperature and for the same duration. Thus, a further increase in green density by slip casting is needed to attain full density and a finer microstructure at lower temperatures. An investigation on the effect of slip casting conditions on densification and the selection of the optimal dopant/co-dopant and sintering conditions, including a two-step sintering method,<sup>6</sup> is now underway.

#### 4. Conclusions

In order to fabricate fine-grained alumina ceramics, Ca-doped (0.1 mol%) alumina nanopowders were prepared through a new sol-gel route using a Ca-doped PHA solution under seeding (5 mass%). The Ca-doped nanopowders thus obtained exhibited excellent sinterability owing to the nano-sized nature of the  $\alpha$ -alumina and developed uniform finer-microstructure due to the suppression effect on grain growth by the homogeneously segregated Ca-dopant to the grain boundaries. The sintered samples attained a relative density of >99% with an average grain size of 0.66  $\mu\text{m}$  at 1375°C by conventional pressureless sintering. This implies that the new sol-gel method, which employs a Ca-doped PHA solution under  $\alpha$ -alumina seeding, would be an effective route for producing nanosized alumina powders, enabling the fabrication of nanocrystalline alumina ceramics at lower sintering temperatures.

#### Reference

1. Nordahl, C. S. and Messing, G. L., Sintering of  $\alpha$ - $\text{Al}_2\text{O}_3$ -seeded

- nanocrystalline  $\gamma$ - $\text{Al}_2\text{O}_3$  powders. *J. Eur. Ceram. Soc.*, 2002, 22, 415-422.
2. Bowen, P., Carry, C., Luxembourg, D. and Hofmann, H., Colloidal processing and sintering of nanosized transition aluminas. *Powder Technol.*, 2005, 157, 100-107.
  3. Hida, M., Yajima, Y., Yamaguchi, T., Taruta, S. and Kitajima, K., Fabrication of submicron alumina ceramics by pulse electric current sintering using  $\text{Mg}^{2+}$ -doped transition alumina powders. *J. Ceram. Soc. Japan*, 2006, 114, 184-188.
  4. Sun, X., Li, J., Zhang, F., Qin, X., Xiu, Z., Ru, H. and You, J., Synthesis of nanocrystalline  $\alpha$ - $\text{Al}_2\text{O}_3$  powders from nanometric ammonium aluminum carbonate hydroxide. *J. Am. Ceram. Soc.*, 2003, 86, 1321-1325.
  5. Huang, C.-L., Wang, J.-J. and Huang, C.-Y., Sintering behavior and microwave dielectric properties of nano alpha-alumina. *Mater. Lett.*, 2005, 59, 3746-3749.
  6. Li, J. and Ye, Y., Densification and grain growth of  $\text{Al}_2\text{O}_3$  nanoceramics during pressureless sintering. *J. Am. Ceram. Soc.*, 2006, 89, 139-143.
  7. Lin, C.-P., Wen, S.-B. and Lee, T.-T., Preparation of nanometer-sized  $\alpha$ -alumina powders by calcining an emulsion of boehmite and oleic acid. *J. Am. Ceram. Soc.*, 2002, 85, 129-133.
  8. Park, Y. K., Tadd, E. H., Zubris, M. and Tannenbaum, R., Size-controlled synthesis of alumina nanoparticles from aluminum alkoxides. *Mater. Res. Bull.*, 2005, 40, 1506-1512.
  9. Li, J., Pan, Y., Xiang, C., Ge, Q. and Guo, J., Low temperature synthesis of ultrafine  $\alpha$ - $\text{Al}_2\text{O}_3$  powder by a simple aqueous sol-gel process. *Ceram. Int.*, 2006, 32, 587-591.
  10. Mazloumi, M., Khalifehzadeh, R., Sadrnezhad, S. K. and Arami, H.,

Alumina nanopowder production from synthetic bayer liquor. *J. Am. Ceram. Soc.*, 2006, 89, 3654-3657.

11. Odaka, A., Yamaguchi, T., Fujita, T., Taruta, S. and Kitajima, K., Cation dopant effect on phase transformation and microstructural evolution in  $M^{2+}$ -substituted  $\gamma$ -alumina powders. *J. Mater. Sci.*, in press.

12. Dynys, F. W. and Halloran, J. W., Alpha alumina formation in alum-derived gamma alumina. *J. Am. Ceram. Soc.*, 1982, 65, 442-448.

13. Tartaj, J., Zárata, J., Tartaj, P. and Lachowski, E. E., Sol-gel cyclic self-production of  $\alpha$ - $Al_2O_3$  nanoseeds as a convenient route for the low cost preparation of dense submicronic alumina sintered monoliths. *Adv. Eng. Mater.*, 2002, 4, 17-21.

14. Yajima, Y., Hida, M., Taruta, S. and Kitajima, K., Pulse electric current sintering and strength of sintered alumina using transition alumina powders prepared from polyhydroxoaluminum gel. *J. Ceram. Soc. Japan*, 2003, 111, 110-116.

15. Yajima, Y., Hida, M., Taruta, S. and Kitajima, K., Pulse electric current sintering and strength of sintered alumina using  $\gamma$ -alumina powders prepared by the sol-gel method. *J. Ceram. Soc. Japan*, 2003, 111, 419-425.

16. Yajima, Y., Yamaguchi, T., Taruta, S. and Kitajima, K., Effect of milling media purity on pulse electric current sintering and strength of alumina ceramics prepared from transition alumina powder. *J. Ceram. Soc. Japan*, 2003, 111, 786-789.

17. Fujita, T., Kitajima, K., Taruta, S. and Takusagawa, N., Chemical species in polyaluminum hydroxide solution. *Nippon Kagaku Kaishi*, 1993, 319-328.

18. Lartigue-Korinek, S., Legros, C., Carry, C. and Herbst, F., Titanium effect on phase transformation and sintering behavior of transition alumina. *J. Eur.*

Ceram. Soc., 2006, 26, 2219-2230.

19. Altay, A. and Gülgün, M. A., Microstructural evolution of calcium-doped  $\alpha$ -alumina. J. Am. Ceram. Soc., 2003, 86, 623-629.

20. Altay, A. and Gülgün, M. A., Calcium in alpha-alumina: the myth and some EM observations. Key Eng. Mater., 2004, 264-268, 219-224.

21. Park, C. W., and Yoon, D. Y., Effects of SiO<sub>2</sub>, CaO<sub>2</sub>, and MgO additions on the grain growth of alumina. J. Am. Ceram. Soc., 2000, 83, 2605-2609.

22. Ahn, J. H., Lee, J.-H., Hong, S.-H., Hwang, N.-M. and Kim, D.-Y., Effect of the liquid-forming additive content on the kinetics of abnormal grain growth in alumina. J. Am. Ceram. Soc., 2003, 86, 1421-1423.

23. Kwon, S. and Messing, G. L., Sintering of mixtures of seeded boehmite and ultrafine  $\alpha$ -alumina. J. Am. Ceram. Soc., 2000, 83, 82-88.

24. Han, K. R., Lim, C. S., Hong, M.-J., Jang, J. W. and Hong, K. S., Preparation method of submicrometer-sized  $\alpha$ -alumina by surface modification of  $\gamma$ -alumina with alumina sol. J. Am. Ceram. Soc., 2000, 83, 750-754.

25. Yen, F. S., Lo, H. S., Wen, H. L. and Yang, R. J.,  $\theta$ - to  $\alpha$ -phase transformation subsystem induced by  $\alpha$ -Al<sub>2</sub>O<sub>3</sub>-seeding in boehmite-derived nano-sized alumina powders. J. Cryst. Growth, 2003, 249, 283-293.

26. Jung, J. and Baik, S., Abnormal grain growth of alumina: CaO effect. J. Am. Ceram. Soc., 2003, 86, 644-649.

## Figure captions

Fig. 1 TEM micrograph of seed powders.

Fig. 2  $\alpha$ -Alumina fraction of the samples plotted against calcination temperature.

○: undoped powder without seeding,  $\Delta$ : undoped powder with 1% seeding,  $\diamond$ : undoped powder with 5% seeding and  $\square$ : Ca-doped powder with 5% seeding.

Fig. 3 TEM micrographs of (a) PA-S and (b) PA-S-Ca powders.

Fig. 4 Bulk density of sintered specimens, plotted against sintering temperature, obtained from PA-S ( $\Delta$ ), PA-S-Ca ( $\circ$ ) and PA-S-Ca(800) ( $\square$ ).

Fig. 5 SEM micrographs of (a) PA-S and (b) PA-S-Ca samples sintered at 1200°C.

Fig. 6 SEM micrographs of PA-S samples sintered at 1350°C (a) and 1400°C (b) and PA-S-Ca samples sintered at 1350°C (c) and 1400°C (d).

Fig. 7 Average grain size plotted against sintering temperature for PA-S ( $\Delta$ ) and PA-S-Ca ( $\circ$ ).



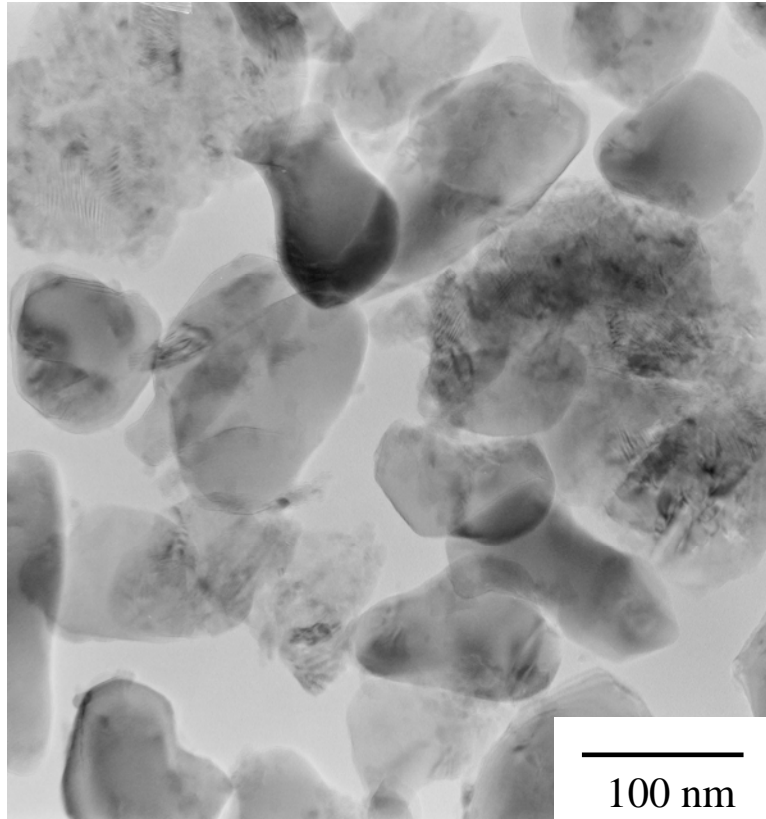


Fig. 1

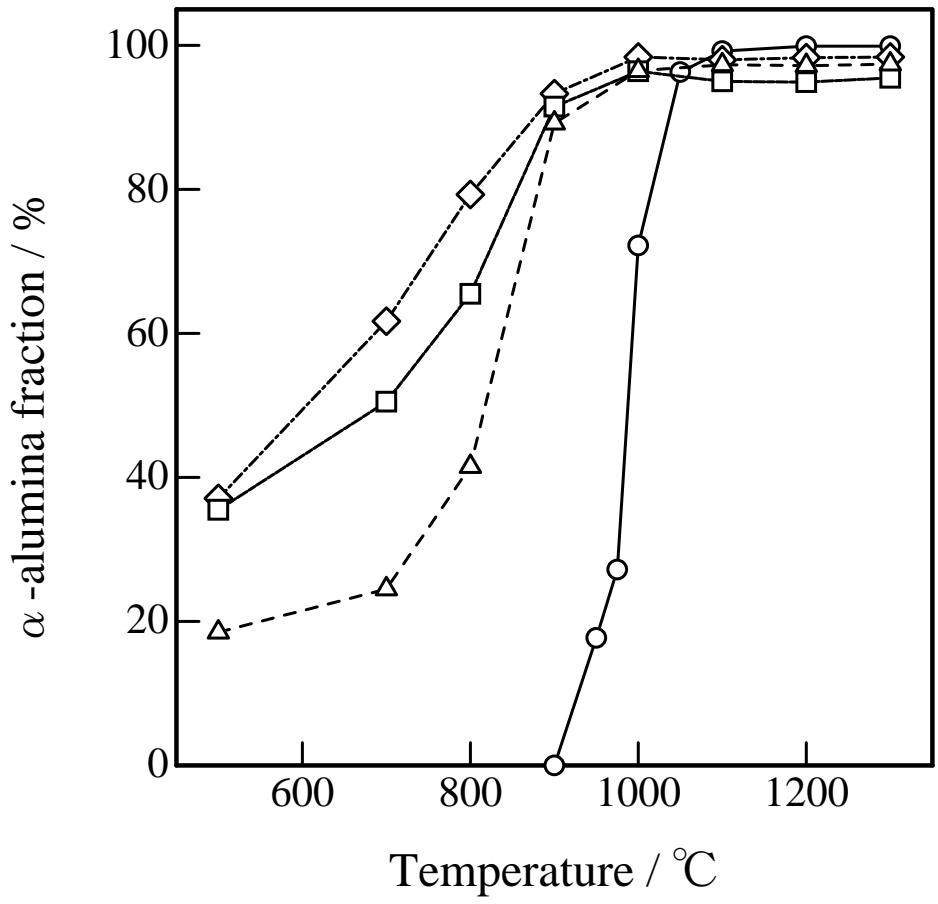


Fig. 2

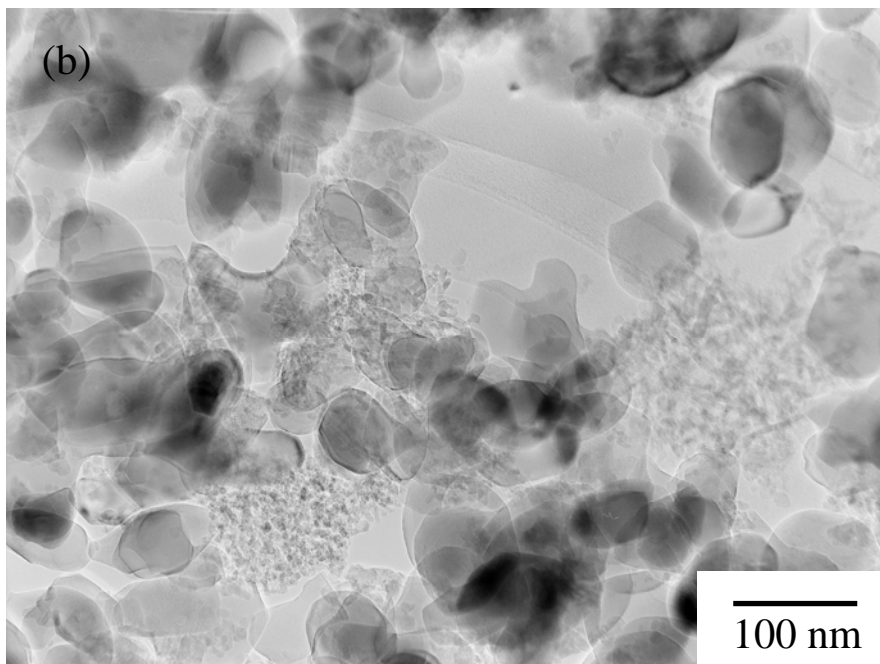
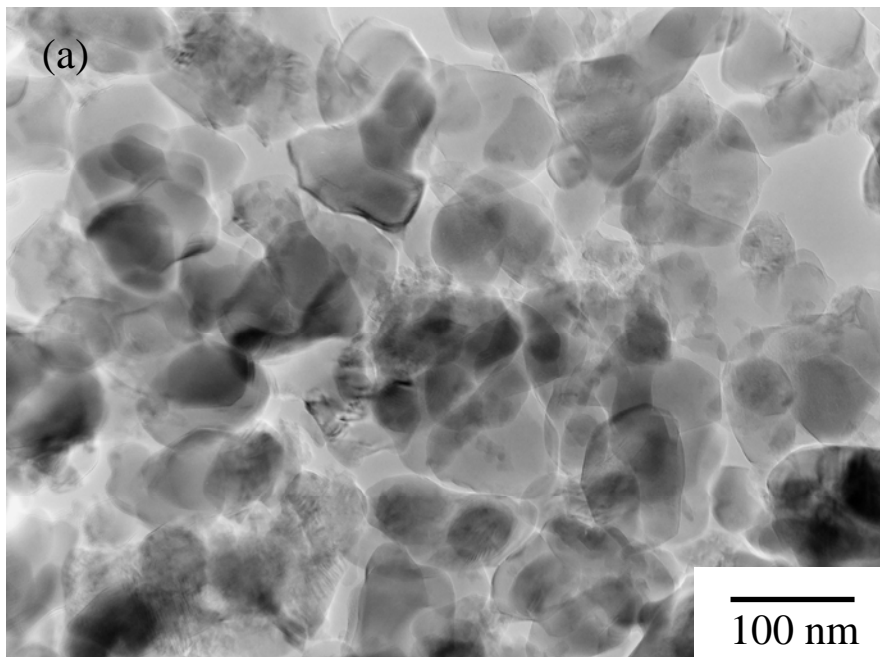


Fig. 3

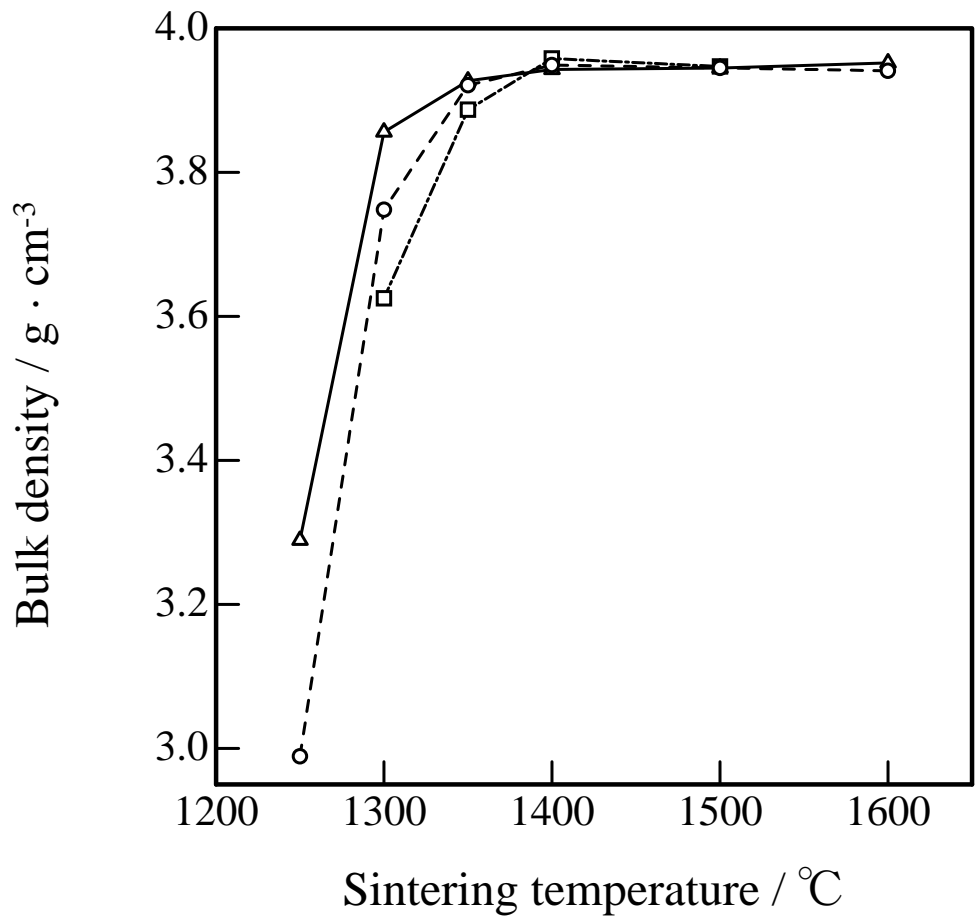


Fig. 4

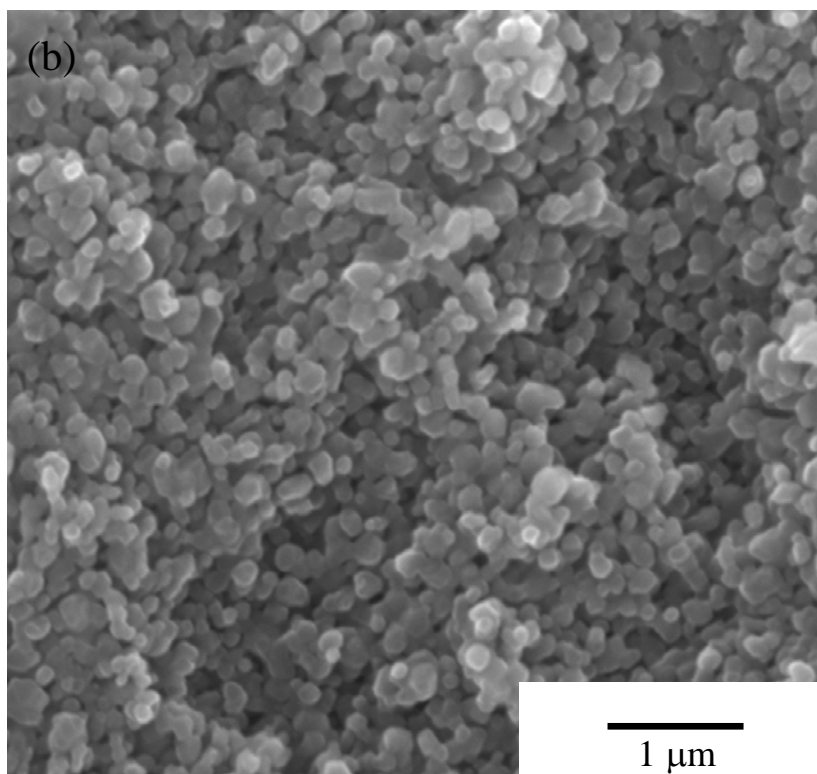
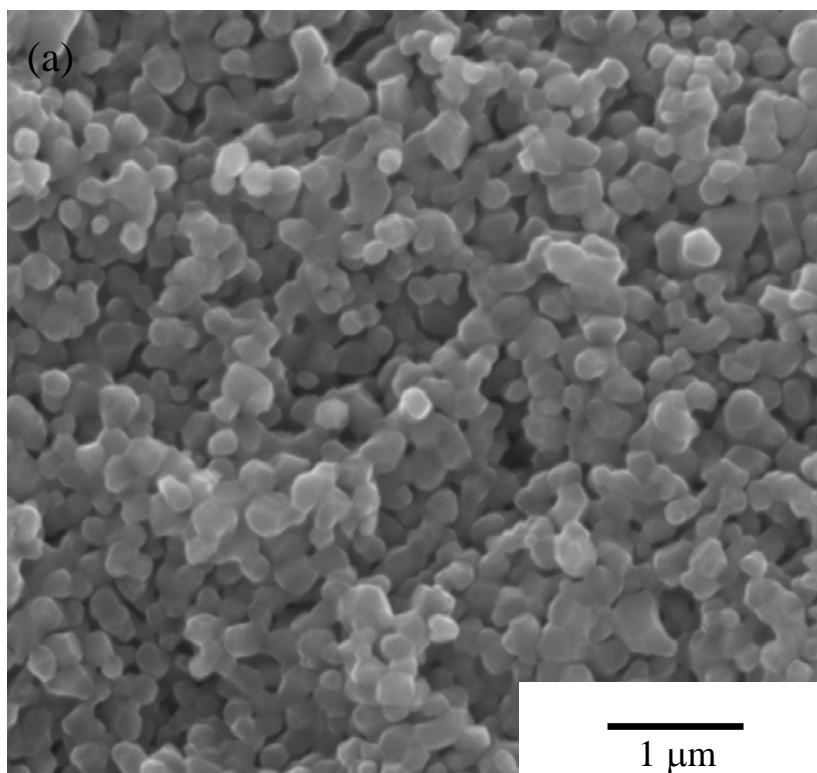


Fig. 5

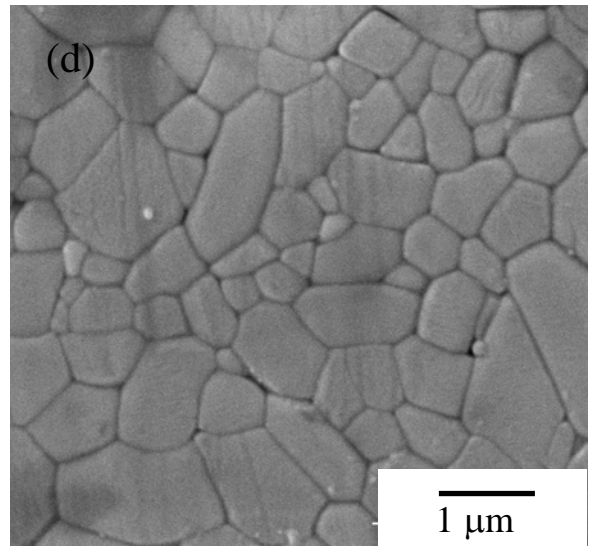
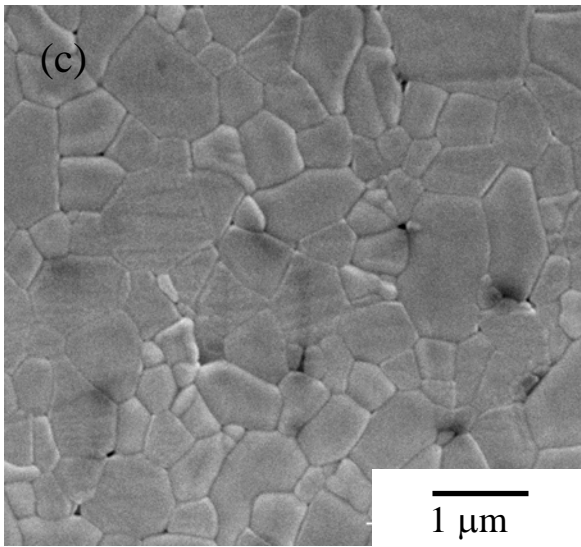
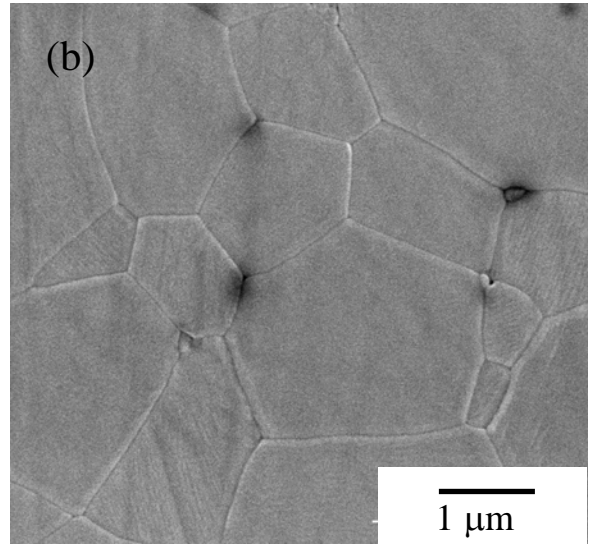
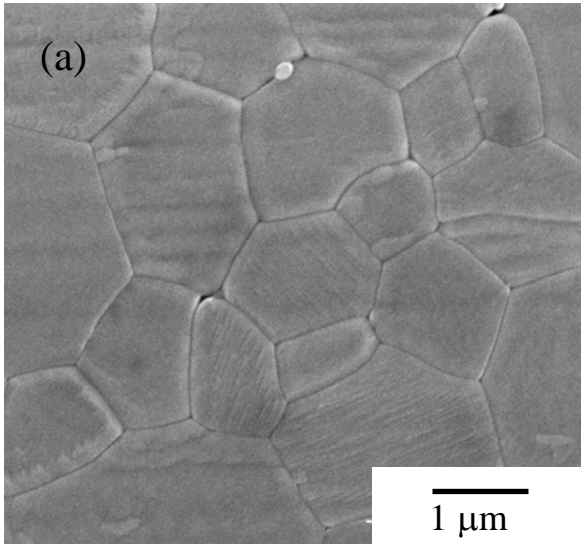


Fig. 6

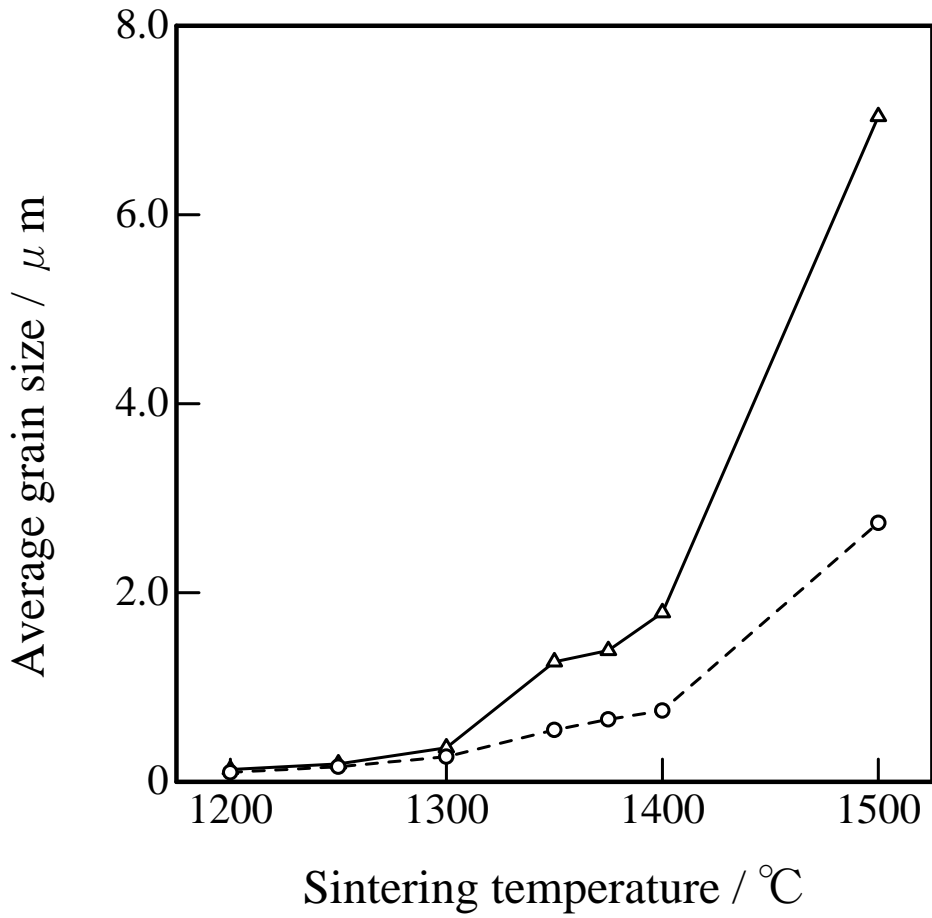


Fig. 7

Table 1 Powder characteristics of the seeds and PA-series samples for sintering.

Sample	Calcination temperature (°C)	BET specific surface area (m <sup>2</sup> /g)	Total pore volume (cm <sup>3</sup> /g)	Mean particle size <sup>a</sup> (nm)	α-fraction (mass%)
PA-S	900	20.1	0.15	75	91
PA-S-Ca	900	20.0	0.14	75	90
PA-S-Ca(800) <sup>b</sup>	800	66.9	0.28	23	65
Seed	-	24.7	0.14	61	100
TM-DAR <sup>c</sup>	-	13.3	0.11	114	100

a: As determined from the specific surface area.

b: Ca-doped alumina powder calcined at 800°C.

c: α-alumina powder used for seeding (before planetary milling).